Optical potentials of halo and weakly bound nuclei

A. Bonaccorso [a,*], F. Carstoiu [b]

[a] *Istituto Nazionale di Fisica Nucleare, Sezione di Pisa, 56100 Pisa, Italy*
[b] *Institute of Atomic Physics, PO Box MG-6, Bucharest, Romania*

Abstract

The optical potential of halo and weakly bound nuclei has a long range part due to the coupling to breakup that damps the elastic scattering angular distributions at all angles for which the effect of the nuclear interaction is felt. In charge exchange reactions leading to a final state with a halo nucleus, the surface potential is responsible for a strong reduction in the absolute cross section. We show how the halo effect can be simply estimated semiclassically and related to the properties of the halo wave function. Assuming an exponential tail for the imaginary surface potential we show that the most important parameter is the diffuseness α of the potential which is directly related to the decay length γ_i of the initial wave function by $\alpha \approx (2\gamma_i)^{-1}$. © 2002 Elsevier Science B.V. All rights reserved.

1. Introduction

In the last years since the advent of Radioactive Beams (RIBs) [1], a new phenomenon called 'nuclear halo' [2] has appeared in nuclear physics. In typical halo nuclei such as ^{11}Be, ^{19}C or ^{8}B [3–11] the valence neutron (proton) or the last couple of neutrons, as in ^{11}Li, occupy weakly bound single-particle states of low angular momentum (s or p). The single-particle wave function of a nucleon halo has a long tail which extends mostly outside the potential well. Then the reactions initiated by such nuclei give large reaction cross sections and neutron breakup cross sections. Also the ejectile parallel momentum distributions following breakup can be very narrow, typically 40–45 MeV/c.

Elastic nucleus–nucleus scattering with a radioactive projectile [12] is another reaction which has been studied to some extent in the attempt to find characteristics that would be typical for a weakly bound nucleus and would help understanding the halo structure. It has

---

* Corresponding author.
 E-mail address: bonaccorso@pi.infn.it (A. Bonaccorso).

been established that the halo breakup is responsible for a damping in the elastic angular distribution in the range 5°–20° about. Recently charge exchange reactions which produce radioactive nuclei in the final state, have also been studied. The effect of the halo breakup is very dramatic in this case, reducing the absolute cross sections by about 50% [13].

All theoretical methods used to describe the above mentioned reactions, require at some stage of the calculation the knowledge of the nucleus–nucleus optical potential. The optical potential is the basic ingredient for the description of elastic scattering, but it is important also in breakup calculations, since we need to take into account the core quasielastic scattering by the target while the halo neutron breaks up. Furthermore in some breakup reactions like those initiated from ^{12}Be or from a core orbital of ^{11}Be it is the ejectile that most likely is going to have a halo structure [14]. In the charge exchange reaction ^{11}B(^{7}Li, ^{7}Be)^{11}Be the halo nucleus–nucleus optical potential necessary to describe the final channel [13] has a volume part obtained with a double folding plus a very diffuse surface term fitted phenomenologically to reproduce the final channel angular distribution.

The problem of the determination of the optical potential for a halo projectile has already been studied by many authors and a review of the present situation can be found in [15]. One method is to start from a phenomenologically determined core–target potential and then the effect of the breakup of the halo neutron is added. This process leads to adding a surface part to the core–target potential. This new surface peaked optical potential has been seen to have a quite long range which should reflect the properties of the long tail of the halo neutron wave function. Such kind of potentials are often called dynamical polarization potentials.

The papers published so far can be divided in two categories: those in which the potential is calculated microscopically [16–22], and those in which it is obtained phenomenologically by fitting elastic or quasielastic data [15,23,24].

In this contribution we propose a new approach to the calculation of the imaginary part of the optical potential due to breakup. It is based on a semiclassical method described by Broglia and Winter in [25,26] and used also by Brink and collaborators [27,28] to calculate the surface optical potential due to transfer and on the Bonaccorso and Brink model for transfer to the continuum reactions [29–33]. The latter is based on the idea that breakup is a reaction following the same dynamics as transfer but leading manly to continuum final states for incident energies per nucleon higher that the average nucleon binding energy. The calculations are almost completely analytical and we will show that a simple approximated formula can be obtained which will help us discussing the origin of the long range nature of the potential and its dependence on the incident energy as well as on the initial neutron binding energy. The characteristics of our potential are consistent with those of potentials obtained with other methods, in particular our theory is close in spirit to the eikonal method of Canto et al. [19] and application to the description of experimental data is encouraging.

2. Theory

The method we will present here is based on the extraction of an optical potential from the calculation of a phase shift.

The elastic scattering probability is $P_{el} = |S_{NN}|^2$, given in terms of the nucleus–nucleus S-matrix. We know that

$$\left| S_{NN}(b) \right|^2 = e^{-4\delta_I(b)}. \tag{1}$$

In a semiclassical approximation [25], the imaginary part of the nucleus–nucleus phase shift δ_I is related to the imaginary part of the optical potential by

$$\delta_I(b) = -\frac{1}{2\hbar} \int\limits_{-\infty}^{+\infty} \left(W_V\big(\boldsymbol{r}(t)\big) + W_S\big(\boldsymbol{r}(t)\big) \right) dt, \tag{2}$$

where the volume potential is responsible for the usual inelastic core–target interaction, while the surface term takes care of the peripheral reactions like transfer and breakup. $\boldsymbol{r}(t) = \boldsymbol{b} + \boldsymbol{v}t$ is the classical trajectory of relative motion for the nucleus–nucleus collision.

According to [25–28] the surface optical potential $W_S(\boldsymbol{r}(t))$ due to transfer can be related to the transfer probability by

$$\int\limits_{-\infty}^{+\infty} W_S\big(\boldsymbol{r}(t)\big) dt = -\frac{\hbar}{2} \sum_{(i,n)} P_n^{(i)}, \tag{3}$$

where $P_n^{(i)}$ are the transfer probabilities in the various channels n. In the traditional formulation the index (i) stands for stripping and pickup to bound states, here we extend it to hold for breakup reactions in which the final neutron state is in the continuum. Breakup of both absorptive and diffractive type will be included. Absorptive breakup has often been called stripping within the halo community. The justification of the use of Eq. (3) to calculate the imaginary potential due to breakup is simply given by the analogy between breakup and transfer as expressed by the transfer to the continuum model introduced in Refs. [29–33]. There it was shown that the formalism for transfer to bound states goes over transfer to the continuum in a natural way if the kinematics of the reaction is taken into account correctly within a time dependent approach which ensures neutron energy conservation.

Using Eqs. (2) and (3), in (1) the nucleus–nucleus S-matrix, in the case of a halo projectile, can be written as

$$|S_{NN}|^2 = |S_{CT}|^2 e^{-P_{b_{up}}}, \tag{4}$$

where S_{CT} takes into account all core–target interactions while the term $e^{-P_{b_{up}}}$ depends only on the halo neutron breakup probability. For a halo nucleus at high incident energy the transfer probability is going to be much smaller than the breakup probability, therefore the surface potential has been identified here with the breakup potential.

In order to obtain the surface imaginary potential equation (3) should be calculated as an identity in the distance of closest approach, which amounts to require that $W_S(r)$ be a local, angular momentum independent function. We remind the reader that since we are using a semiclassical method, the nonlocality, which is in principle a characteristic of microscopic optical potentials has been transformed into an energy dependence [34].

Now we discuss the hypothesis leading to Eq. (4). The reactions with halo projectiles we are concerned with in this paper have been performed at energies well above the Coulomb

barrier where many inelastic channels open at about the same distance of closest approach. The effect of the breakup is most important at large distances ($b > R_s$) of closest approach, where it represents the dominant reaction mechanism. If the breakup probability is needed at smaller impact parameters, then the values calculated by perturbation theory, have to be multiplied by the core survival probability, as discussed in Eq. (V.8.1) of Broglia and Winther [25] and also used in relation to halo breakup by several authors. The effect of all inelastic channels n different from the one we are interested in, can be taken into account by introducing a damping factor P_0. Therefore the breakup probability P_{b_up} at all distances can be defined as

$$P_{b_\mathrm{up}} = p_{b_\mathrm{up}} \prod_n (1 - p_n) \approx p_{b_\mathrm{up}} \exp\left(-\sum_n p_n\right) = p_{b_\mathrm{up}} P_0. \tag{5}$$

Each elementary inelastic probability p_n and breakup probability p_{b_up} is small and p_{b_up} in particular, can be calculated in time dependent perturbation theory, as done in [29]. In this paper we will treat only the nuclear breakup channels, which are important for light targets. In the case of heavy targets also the Coulomb breakup has to be taken into account.

In reactions with halo projectiles the damping factor P_0 has also been referred to as the core survival probability after the halo breakup or as the core elastic scattering probability. The breakup probability Eq. (5) integrated over the impact parameter b has been widely used in the literature to get total breakup cross sections.

The breakup probability p_{b_up} with the index b_up standing for one neutron breakup can be obtained by integrating the neutron energy or momentum spectrum as given, for example, in [33]:

$$p_{b_\mathrm{up}} \approx \int \mathrm{d}\varepsilon_f \sum_{l_f} \left(\left|1 - \langle S_{l_f} \rangle\right|^2 + 1 - \left|\langle S_{l_f} \rangle\right|^2 \right) B(l_f, l_i). \tag{6}$$

It is important to remark that the above expression takes into account to all orders the neutron target final state interaction via an energy and angular momentum dependent optical model wave function of the breakup neutron. In this way neutron elastic scattering and absorption are treated consistently via an unitary S-matrix. Eq. (6) is the neutron transfer probability from a definite single-particle state of energy ε_i, momentum $\gamma_i = \sqrt{-2m\varepsilon_i}/\hbar$, and angular momentum l_i in the projectile to all possible final continuum states of energy ε_f, momentum $k_f = \sqrt{2m\varepsilon_f}/\hbar$. It is the sum of the transfer probabilities to each possible final l_f-state for a given final energy ε_f. In Ref. [30] it was shown that the first term of Eq. (6), proportional to $|1 - \langle S_{l_f} \rangle|^2$, gives the neutron elastic breakup spectrum while the second term proportional to the transmission coefficient $T = 1 - |\langle S_{l_f} \rangle|^2$ gives the absorption spectrum. This term contains contributions from inelastic scattering of the breakup neutron by the target nucleus and also from compound nucleus formation.

The factor $B(l_f, l_i)$ is an elementary transfer probability which depends on the details of the initial and final states, on the energy of relative motion and on the distance of closest approach b between the two nuclei. Its explicit expression reads:

$$B_{l_f, l_i} = \frac{1}{2}\left[\frac{\hbar}{mv}\right]^2 \frac{m}{\hbar^2 k_f} (2l_f + 1)|C_i|^2 \frac{\mathrm{e}^{-2\eta b}}{2\eta b} P_{l_i}(X_i) P_{l_f}(X_f), \tag{7}$$

where

$$X_i = 2(\eta/\gamma_i)^2 - 1, \qquad X_f = 2(\eta/k_f)^2 + 1.$$

Also

$$k_1 = -\frac{\varepsilon_i - \varepsilon_f + \frac{1}{2}mv^2}{\hbar v} \quad \text{and} \quad k_2 = -\frac{\varepsilon_i - \varepsilon_f - \frac{1}{2}mv^2}{\hbar v}$$

are the z components of the neutron momentum in the initial and final state, respectively. $\eta^2 = k_1^2 + \gamma_i^2 = k_2^2 - k_f^2$ is the modulus square of the transverse component of the neutron momentum. $mv^2/2$ is the incident energy per nucleon at the distance of closest approach b for the ion–ion collision. $|C_i|^2$ is the asymptotic normalization constant of the initial state wave function and P_{l_i} and P_{l_f} are Legendre polynomials coming from the angular parts of the initial and final wave functions, respectively, [29]. Coulomb breakup can be taken into account as well, following the formalism of [37]. One advantage of calculating the breakup probability by Eq. (7) is that no sudden approximation hypothesis is made and thus the method is valid for any initial separation energy.

In Eq. (6) the main dependence on the core–target distance of closest approach b is contained in the exponential factor $e^{-2\eta b}$. Equation (7) has a maximum in correspondence to the minimum value of $\eta = \gamma_i$. Therefore after integrating over ε_f the b-dependence of the breakup probability $p_{b_{up}}(b)$ will still be of the exponential form $p_{b_{up}}(b) \approx e^{-b/\alpha}$ with $\alpha \approx (2\gamma_i)^{-1}$ where γ_i is the decay length of the neutron initial state wave function. We now assume at large distances, where $P_0 = 1$ the same exponential dependence for the absorptive potential, $W_S(r) = W_0 e^{-r/\alpha}$ and as indicated earlier on, a straight line parameterization for the trajectory $\boldsymbol{r}(t) = \boldsymbol{b} + \boldsymbol{v}t$, then Eq. (3) reads:

$$\int\limits_{-\infty}^{+\infty} W_S(b, z)\, dz = -\frac{\hbar v}{2} p_{b_{up}}(b). \tag{8}$$

The LHS can be approximately evaluated as

$$\int\limits_{-\infty}^{+\infty} W_S(b, z)\, dz = W_0 \int\limits_{-\infty}^{+\infty} e^{-(b + \frac{z^2}{2b})/\alpha}\, dz = W_0 \sqrt{2\pi b\alpha}\, e^{-b/\alpha}, \tag{9}$$

where we assumed $b \gg z$ in the second step. Equating the RHS of Eqs. (8) and (9) and renaming the distance b as r gives

$$W_S(r) = -\frac{\hbar v}{2} p_{b_{up}}(r) \frac{1}{\sqrt{2\pi\alpha r}}. \tag{10}$$

The exponential form of $W_S(r)$ implies that the strength of the breakup potential be a function of r. However we know that in nuclear induced peripheral reactions like breakup and transfer most of the cross section comes from impact parameters around the strong absorption radius. Therefore writing $p_{b_{up}}(r) \approx p_{b_{up}}(R_s) e^{-(r - R_s)/\alpha}$ we finally get that Eq. (10) can be written as

$$W_S(r) \approx W_0 e^{-\frac{r - R_s}{\alpha}}, \tag{11}$$

where

$$W_0 \equiv W_0(R_s) = -\frac{\hbar v}{2} p_{b_{up}}(R_s) \frac{1}{\sqrt{2\pi \alpha R_s}}, \tag{12}$$

which gives an estimate of the strength parameter of the surface breakup potential at the typical distance R_s.

Equation (11) has a number of interesting features. First of all it shows explicitly that the long range nature of the breakup potential originates from the large decay length of the initial state wave function. For a typical halo separation energy of 0.5 MeV, $\alpha = (2\gamma_i)^{-1} = 3.2$ fm, while for a 'normal' binding energy of 10 MeV, $\alpha = 0.7$ fm as expected. Therefore the parameter α will depend only on the projectile characteristics and not on the target. Furthermore looking at Eqs. (11) and (12) we notice that for a fixed initial state the strength of the potential will be larger the smaller the neutron binding energy. On the other hand, for a fixed binding energy the potential strength will be lower the higher the initial angular momentum. Finally the strength parameter W_0 is seen to be energy dependent from different sources. If we consider R_s, the typical distance at which the strength is calculated, to be the same at all energies, then the energy dependence of W_0 is given by its linear dependence on the velocity of relative motion v, which is a function of the projectile–target combination. Another energy dependence is trough the breakup probability, whose behaviour in turn is determined in part by the neutron–target energy dependent optical potential. At the large distances we are interested in, the overall energy dependence of the breakup probability is an exponential decrease with incident energy due to the dependence on v and on the neutron–target optical potential. Therefore W_0 is expected to rise up to about $40\,A$ MeV and then to decrease at higher energies. Another interesting way to look at the behaviour of the strength W_0 is to consider instead explicitly that the strong absorption radius R_s is itself decreasing with energy. If we take this dependence into account, then W_0 increases up to about $80\,A$ MeV and then starts to decrease. However the precise energy dependence of R_s requires an accurate knowledge of the energy dependence of the core–target volume optical potential. This is beyond the scope of the present work, therefore we will discuss the energy dependence of the surface potential at a fixed distance large enough to have unit core survival probability at all incident energies.

It is very well known that the dynamical polarization potential due to surface reactions gives rise also to a correction to the real part of the nucleus–nucleus optical potential. In terms of Feshbach potential both the real and imaginary parts of the dynamical polarization potential come from the second order term and therefore the real polarization term gives a correction to the first order term, which is purely real and it is often referred to as the folding potential. The relative magnitude of this correction with respect to the first order real potential depends on the system involved and on the incident energy. One characteristic of the real dynamical potential, discussed by many authors is to become repulsive at some energies. The imaginary polarization potential on the other hand is by definition negative from Eq. (10). The real dynamical potential is expected to have the same exponential dependence as the imaginary part. The simple and consistent way we have used here to obtain its strength is by applying a dispersion relation.

2.1. Dispersion relation

The theoretical optical potential is highly nonlocal and energy dependent. In most applications it is replaced by an equivalent local potential

$$U(r, E) = V_R(r, E) + \Delta V(r, E) + iW(r, E).$$

The term V_R is usually associated with the folding potential and contains a spurious energy dependence due to the finite range of the underlying nucleon–nucleon effective interaction and Pauli principle. We have further assumed that the imaginary potential splits into contributions coming from coupling to breakup (W_S) and other inelastic excitations (W_V) so that

$$W(r, E) = W_V(r, E) + W_S(r, E).$$

The real part of the dynamic polarization potential (DPP) arising from coupling of elastic channel to the breakup is calculated from the dispersion relation

$$\Delta V(r, E) = \frac{P}{\pi} \int\limits_0^\infty \frac{W_S(r, E') \, dE'}{E' - E}. \tag{13}$$

The numerical evaluation of this term requires the knowledge of the imaginary potential at all energies. Our model provides accurate values in a limited range of energies $E < 1600$ MeV for which the nucleon–target potential is known with reasonable accuracy. At higher energies we assume a reasonable energy dependence of the form $W_S \sim E^{-1}$ in such a way that the integral in Eq. (13) converges and it can be evaluated accurately for the energies of interest. An algebraic exact model similar to that used in [35] has been used to check the numerical accuracy.

3. Results

In order to sample the quantitative accuracy of the simple analytical model presented above we discuss now some numerical examples. The potentials we will discuss derive from the breakup of the $2s_{1/2}$ and $1p_{1/2}$ states of ^{11}Be, with separation energies 0.5 and 0.18 MeV, respectively. It has been shown that during the charge exchange reaction of [13], ^{11}Be can be populated in the final channel in either the ground state or the first $1/2^-$ excited state. There are in the literature a number of papers discussing the breakup potential for a ^{11}Li projectile, among others [15,18,19,22]. ^{11}Be breakup from the $2s$ has been discussed in [20,21]. However the potential due to breakup of the $1p_{1/2}$ bound excited state has never been discussed before.

The neutron–target optical potential used here to calculate the breakup probabilities is the same as in [36]. The core survival probability has been parameterized as

$$P_0(b) = |S_{CT}|^2 = \exp\left(-\ln 2 e^{[(R_s-b)/a]}\right), \tag{14}$$

where $a = 0.6$ fm and the strong absorption radius $R_s = 1.4(A_P^{1/3} + A_T^{1/3})$ fm.
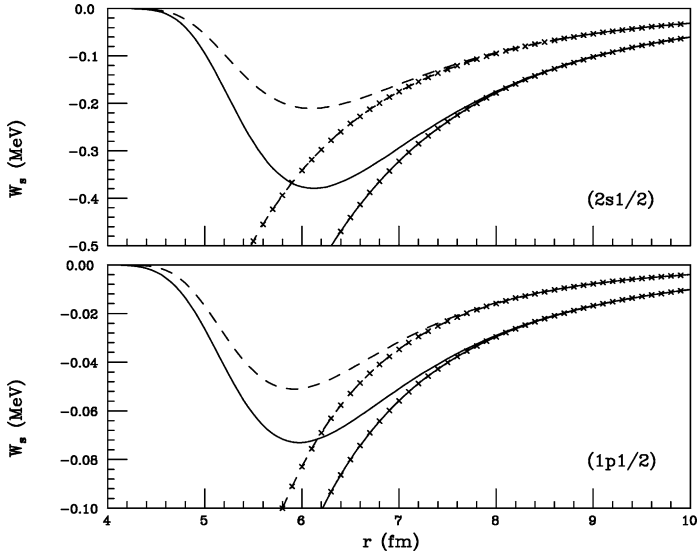
Fig. 1. Radial shape of the surface imaginary potential for the system ^{7}Be + ^{11}Be due to breakup from the $2s$ and $1p_{1/2}$ states of ^{11}Be at $E = 57$ MeV (dashed lines) and $E = 550$ MeV (solid lines). Lines with symbols are calculated assuming $P_0 = 1$ in Eqs. (3) and (5).

We start by showing in Fig. 1 the radial shapes of the potentials calculated for the breakup from the $2s$ and $1p_{1/2}$ states of ^{11}Be in the interaction with ^{7}Be relevant to the charge exchange reaction of [13]. In both figures we show results for two laboratory scattering energies for the ion–ion system: $E = 57$ MeV (dashed lines) and $E = 550$ MeV (solid lines). The lines with symbols correspond to the exponential approximation for the potentials, Eqs. (10)–(12) while the lines without symbols are obtained from Eq. (10) using for the breakup probability the $P_{b_{up}} \approx p_{b_{up}} P_0$ definition valid at all distances. Our results show a strong dependence of the potential on the incident energy (compare solid and dashed lines) and also a quite strong state dependence. In fact in the case of the s-state the diffuseness of the potential is about 2.3 fm, while for the p-state is about 2 fm while the strength for the s-state is about five times more than for the p-state although the binding energy is larger. This is due to the fact that for $l > 0$ states the effect of the centrifugal barrier hinders breakup. The values of the diffuseness are slightly smaller than the estimate given in Section 2 because of the integration over the neutron final energy of the breakup probability. Finally we would like to stress that the internal part of the surface polarization potential has no effect on the nucleus–nucleus scattering as it can be seen also from the nucleus–nucleus S-matrix of Fig. 2 which we are going to discuss next.

Another important application is in fact to see how the elastic scattering total probability changes as a function of the impact parameter or angular momentum when there is a strong breakup probability. In Fig. 2 we show the core–target S-matrix, S_{CT} of Eq. (14) (solid line) and the nucleus–nucleus S-matrix S_{NN} (dashed line) from Eq. (4), calculated with $P_{b_{up}} = p_{b_{up}}$, which contains the effect of the halo breakup. In this case the exponential approximation for the surface potential is used at all distances. At a fixed impact parameter
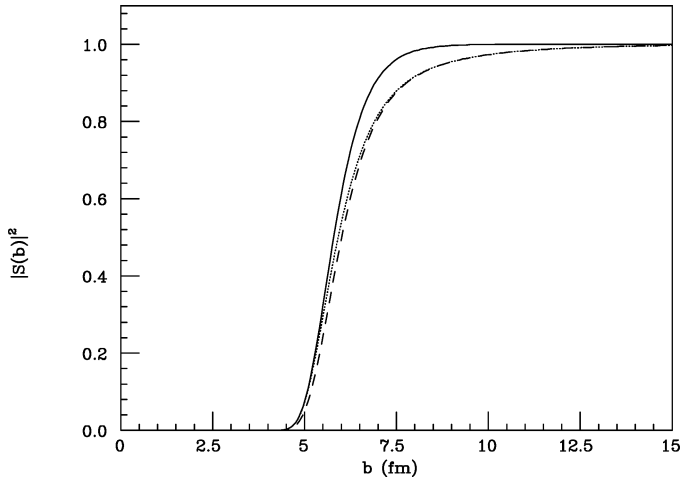
Fig. 2. S-matrix values as a function of the impact parameter for the system $^{11}\text{Be} + {}^9\text{Be}$ at $50\,A$ MeV. Solid line is $|S_{\text{CT}}|^2$, dashed and dotted lines are $|S_{\text{NN}}|^2$ calculated with the two prescriptions for the breakup probability discussed in the text.

(or angular momentum) the effect of the breakup is to reduce the elastic probability given by the modulus square of the S-matrix. The unitarity limit is attained at much larger b-values and the reaction cross section receives significant contributions from a large range of impact parameters. This result is analogous to the discussion reported in [14]. The reduction is more pronounced at the impact parameters larger than the strong absorption radius. The value of the strong absorption radius does not change appreciably because it is mainly determined by the core–target interaction which is strongly absorptive. On the other hand, it is in a sense obvious that surface reactions such as breakup would change the S-matrix behaviour at large impact parameters where they represent the dominant reaction channels.

The dotted line is the S-matrix also calculated from Eq. (4) but this time we have used $P_{b_{\text{up}}} = p_{b_{\text{up}}} P_0$ with P_0 given by Eq. (14). With this prescription one gets an imaginary breakup potential valid at all distances. The fact that the two S-matrices (dashed and dotted line) are hardly distinguishable is a proof of the fact that elastic scattering is not sensitive to the internal part of the polarization potential.

Fig. 3 contains the energy dependence of the imaginary and real strengths of the dynamical polarization potential due to breakup of the halo neutron in the reaction $^{11}\text{Be} + {}^9\text{Be}$. The solid line gives the energy dependence of the imaginary potential calculated at the fixed distance 7 fm which is slightly larger than the sum of the projectile and target radii. This distance is about the smallest at which absorption into channels other than breakup can be neglected and the core survival probability is $P_0 = 1$. The real part of the potential obtained from the dispersion relation is given by the dashed line. It shows a change of sign which gives a repulsive real potential from around the energy ($70\,A$ MeV) at which the imaginary part starts to have a clear decrease toward zero. This is the obvious and consistent result of having applied the dispersion relation. Physically it means that the
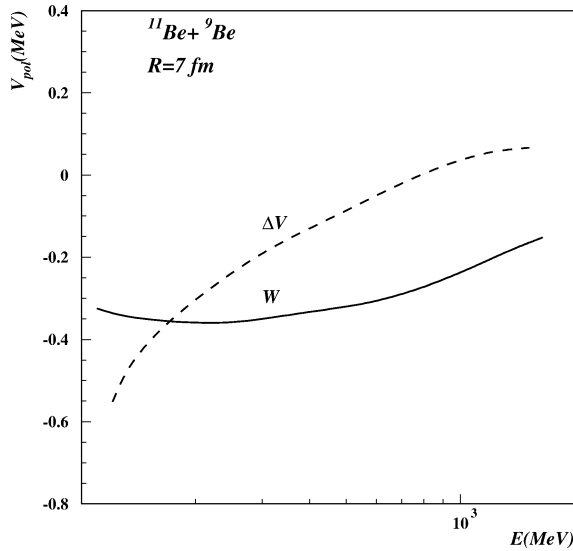
Fig. 3. Energy dependence of the strengths of real and imaginary polarization potential for the system ^{11}Be $+ ^9$Be at the distance 7 fm.

mean field will prevent from entering the interaction region those waves that cannot be absorbed.

Since the optical potential has one of its most interesting application in the calculation of elastic scattering angular distributions, we finally show in Fig. 4(a) an example for the reaction ^{11}Be $+ ^{12}$C at 49.3 A MeV. The data are from P. Russel-Chomaz et al. [39]. The optical model parameters for the volume parts of the bare potential are taken from [21] and were fitted to ^{10}Be elastic scattering data at 59.4 A MeV. They are:

$$V_R = 123 \text{ MeV}, \qquad r_R = 0.75 \text{ fm}, \qquad a_R = 0.8 \text{ fm},$$
$$W_V = 65 \text{ MeV}, \qquad r_I = 0.78 \text{ fm}, \qquad a_I = 0.8 \text{ fm}.$$

In our case we have defined the real and imaginary radii by multiplying the radius parameters by $(11^{1/3} + 12^{1/3})$, in order to take into account in the volume potential the presence of the extra neutron with respect to the core. The consequences of this choice are discussed in the following in relation to Fig. 4(b).

In Fig. 4(a) the solid line is the calculation with the bare volume potential. The dashed line is obtained instead including the surface imaginary potential calculated according to the method proposed in this work. The large diffusivity in the breakup absorption leads to changes in the S-matrix in all partial waves as discussed above and the angular distribution is damped. The inclusion of the real polarization potential (dotted line) gives a negligible modification to the quality of the fit since its strength (-0.15 MeV) at this incident energy (50 A MeV) is very small with respect to the volume part. Also variations in the strength of the imaginary surface potential up to about 30% result in negligible differences in the angular distribution. As expected the effect of breakup is to suppress scattering at all angles larger than about 5°. The angular distribution shows the usual Fraunhofer oscillations at
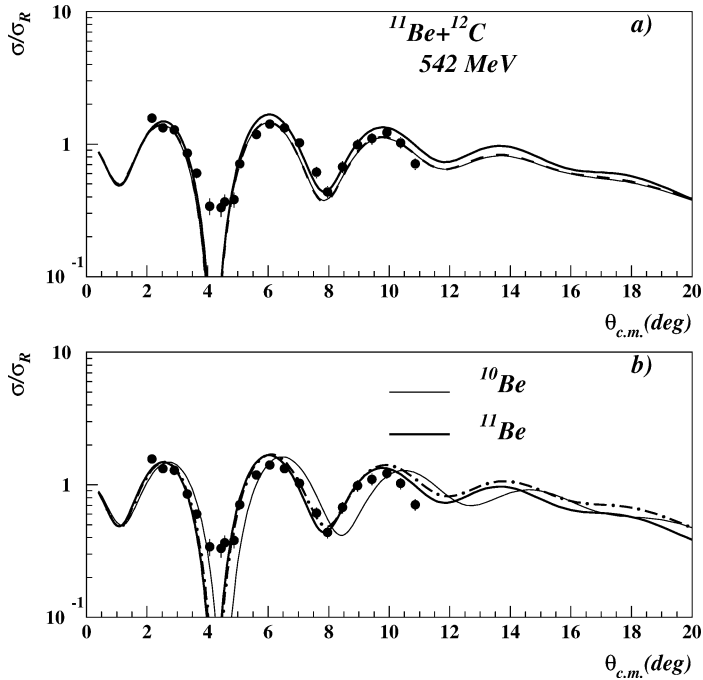
Fig. 4. (a) Elastic scattering angular distribution for the reaction ^{11}Be + ^{12}C. Solid line is with a bare volume imaginary potential. Dashed line is obtained adding the imaginary surface potential calculated in this work. Dotted line includes also the real part of the surface potential. (b) Solid line is obtained with the same bare potential as in (a), the dotted line is obtained by decreasing both the real and imaginary potential radii as explained in the text, while the dot-dashed line is obtained decreasing only the imaginary potential radius.

small angles followed by an almost exponential decrease of the cross section due to a far side dominance. No Airy like oscillation are seen since the absorption is already too strong.

In order to clarify the dependence of the calculated angular distribution on the choice of the radius parameters of the bare potential, in Fig. 4(b) we show again the data and the angular distribution with the bare potential as in Fig. 4(a) (full line), plus the angular distribution with the bare potential in which the radii have been calculated from the above radius parameters but multiplied by $(10^{1/3} + 12^{1/3})$ (dotted line). This is to show that, as expected, a small decrease in the radius of the optical potential would give a slight shift toward larger angles. With the dot-dashed line we show instead the calculation done with the radii chosen as

$$R_R = r_R\left(11^{1/3} + 12^{1/3}\right) \text{ fm} \quad \text{and} \quad R_I = r_I\left(10^{1/3} + 12^{1/3}\right) \text{ fm}.$$

This calculation agrees very well with the full line calculation up to about 10°. For larger angles only a change in the magnitude of the cross section is seen while there is no shift in the peak position, which is then determined by the radius of the real volume potential.

Another significant effect of the imaginary surface potential is seen in the calculated total reaction cross section given in Table 1. We obtain an increase of 150 mb with respect to the bare (no breakup) optical potential mainly due to an increase of about 10% in the

Table 1
Volume integrals per number of interacting nucleon pairs and rms radii of the Woods–Saxon potential used in Fig. 2 for ^{11}Be + ^{12}C scattering

Pot.	J_{V_R} [MeV fm^3]	R_{V_R} [fm]	J_W [MeV fm^3]	R_W [fm]	σ_{NN} [mb]
V_{opt}	235	3.964	145.6	4.257	1255
$V_{opt} + iW_S$	235	3.964	151.7	4.598	1399

The last column gives the total reaction cross section. Here $V_{opt} = V_R + iW_V$.

rms radius and 5% in the volume integral of the absorption. The increase in the reaction cross section is very close to the total breakup cross section $\sigma_{b_{up}} \approx 170$ mb expected at this energy [38]. This is consistent with the hypothesis that $P_{b_{up}}$ is small in Eq. (4). In fact expanding the exponential in Eq. (4) to first order in $P_{b_{up}}$ and integrating over the impact parameter b one immediately finds

$$\sigma_{NN} \approx \sigma_{CT} + \sigma_{b_{up}}. \tag{15}$$

In the case of the charge exchange reaction the effect of the surface breakup potential is more dramatic, giving a decrease in the cross section of about 50% [13] necessary to fit the data.

4. Conclusions

In conclusion we have presented a simple analytical method to obtain the surface component of the real and imaginary parts of the nucleus–nucleus optical potential in the case in which one partner of the reaction is a halo or weakly bound nucleus. The main purpose here was to relate the characteristics of the potential to the special properties of the breakup channel for weakly bound nuclei. The evaluation of the potential amounts in fact just to the calculation of the breakup probability. If breakup from core excited states is to be included, then it suffices to sum up the relative probabilities according to Eq. (3).

The method is an extension of that previously used to calculate microscopically the effect of transfer channels on the imaginary potential. The shape of the surface imaginary potential and its parameters are determined univocally by the shape of the breakup form factor. An interesting result is that the diffuseness of the potential reflects the decay length of the neutron wave function entering breakup and therefore depends mainly upon the projectile characteristics, but in a model independent way. The strength parameter has a rather complicated but physically understandable energy dependence which we have discussed. At a given distance the uncertainty on the strength would be of about 30%, reflecting mainly the model dependence of the breakup probability values [36]. The real potential has been obtained via the use of a dispersion relation and shows the interesting property of becoming repulsive when the imaginary part starts to decrease due to the closing up of the breakup channel when the energy becomes too high. Sample calculations have shown that the potential proposed here is consistent with other theoretical models Refs. [18,19,21] for similar, light halo systems and also with existing experimental data. Furthermore we have given an explicit justification for the long range of the polarization potential as coming from the small decay length of the initial neutron wave function.

References

[1] I. Tanihata et al., Phys. Lett. B 160 (1985) 380.
[2] P.G. Hansen, A.S. Jensen, B. Jonson, Annu. Rev. Nucl. Part. Sci. 45 (1995) 591, and references therein.
[3] W. Schwab et al., Z. Phys. A 350 (1995) 238.
[4] I. Pecina et al., Phys. Rev. C 52 (1995) 191.
[5] F. Negoita et al., Phys. Rev. C 54 (1996) 1787.
[6] D. Bazin et al., Phys. Rev. Lett. 74 (1995) 3569.
[7] D. Bazin et al., Phys. Rev. C 57 (1998) 2156.
[8] A. Bonaccorso, Phys. Rev. C 60 (1999) 054604.
[9] T. Nakamura et al., Phys. Rev. Lett. 83 (1999) 1112.
[10] V. Maddalena et al., Phys. Rev. C 63 (2001) 024613, and references therein.
[11] V. Maddalena, R. Shyam, Phys. Rev. C 63 (2001) 051601.
[12] J.J. Kolata et al., Phys. Rev. Lett. 69 (1992) 2631;
   M. Lewitowicz et al., Nucl. Phys. A 562 (1993) 301;
   W. Mittig, P. Roussel-Chomaz, Nucl. Phys. A 693 (2001) 495, and references therein.
[13] F. Cappuzzello et al., Phys. Lett. B 516 (2001) 21, and private communication.
[14] J.A. Tostevin, J. Phys. G 25 (1999) 735.
[15] J.C. Pacheco, N. Vinh Mau, Nucl. Phys. A 669 (2000) 135.
[16] N. Takigawa et al., Phys. Lett. B 288 (1992) 244.
[17] Y. Sakuragi, S. Funada, Y. Hirabayashi, Nucl. Phys. A 588 (1995) 65c.
[18] K. Yabana, Y. Ogawa, Y. Suzuki, Nucl. Phys. A 539 (1992) 295;
   K. Yabana, Y. Ogawa, Y. Suzuki, Phys. Rev. C 45 (1992) 2909.
[19] L.F. Canto, R. Donangelo, M.S. Hussein, M.P. Pato, Nucl. Phys. A 542 (1992) 131;
   F. Canto, R. Donangelo, M.S. Hussein, Nucl. Phys. A 529 (1991) 243.
[20] R.C. Johnson, J.S. Al-Khalili, J.A. Tostevin, Phys. Rev. Lett. 79 (1997) 2771.
[21] J.S. Al-Khalili, J.A. Tostevin, J.M. Brooke, Phys. Rev. C 55, R1018.
[22] J.S. Al-Khalili, Nucl. Phys. A 581 (1995) 315.
[23] M.S. Hussein, G.R. Satchler, Nucl. Phys. A 567 (1994) 165.
[24] D.T. Khoa, G.R. Satchler, W. von Oertzen, Phys. Lett. B 358 (1995) 14.
[25] R.A. Broglia, A. Winther, Heavy Ion Reactions, Benjamin, Reading, MA, 1981.
[26] R.A. Broglia, G. Pollarolo, A. Winther, Nucl. Phys. A 361 (1981) 307.
[27] A. Bonaccorso, G. Piccolo, D.M. Brink, Nucl. Phys. A 441 (1985) 555.
[28] Fl. Stancu, D.M. Brink, Phys. Rev. C 32 (1985) 1937.
[29] A. Bonaccorso, D.M. Brink, Phys. Rev. C 38 (1988) 1776.
[30] A. Bonaccorso, D.M. Brink, Phys. Rev. C 43 (1991) 299.
[31] A. Bonaccorso, D.M. Brink, Phys. Rev. C 44 (1991) 1559.
[32] A. Bonaccorso, D.M. Brink, Phys. Rev. C 46 (1992) 700.
[33] A. Bonaccorso, D.M. Brink, Phys. Rev. C 58 (1998) 2864.
[34] A. Bonaccorso, D.M. Brink, Nucl. Phys. A 384 (1982) 161.
[35] C. Mahaux, H. Ngô, G.R. Satchler, Nucl. Phys. A 449 (1986) 354.
[36] A. Bonaccorso, G.F. Bertsch, Phys. Rev. C 63 (2001) 044604.
[37] J. Margueron, A. Bonaccorso, D.M. Brink, Nucl. Phys. A (2002).
[38] A. Bonaccorso, F. Carstoiu, Phys. Rev. C 61 (2000) 034605.
[39] P. Russel-Chomaz et al., private communication.